

## Removal of Hazardous Methylene Blue from Aqueous Solutions by Green Citrus Mold (*Penicillium digitatum*)@Chitosan Hydrogel Beads

### ABSTRACT

**Objective:** This research focuses on the novel technique of using green citrus mould (GCM), namely *Penicillium digitatum*, in conjunction with chitosan (Ctsn) as a composite to extract Methylene Blue (MB) from aqueous solutions and the composite-dye interactions were assessed analytically.

**Methods:** FT-IR and EDX were used to analyze the chemical characteristics of the adsorbent surface. SEM was used to visualize surface morphology. Kinetic studies were carried out for the removal of MB dye from aqueous solution with the synthesized biosorbent, equilibrium isotherms were derived and adsorption mechanism was investigated. The isotherm parameters of biosorption were determined using the most widely used adsorption models.

**Results:**  $Q_{max}$  value of Green Citrus Mold @Chitosan Hydrogel Beads (GCM@Ctsn) from Langmuir isotherm parameters was calculated as 60.24 mg/g. The dosage of adsorbent that performed optimally was found to be 2 g/L. The pH range, between pH 6 and pH 8, was shown to be the optimal range for attaining optimum removal effectiveness. The thermodynamic data indicated that an exothermic, spontaneous reaction occurred between the MB molecules and the composite.

**Conclusion:** The results highlight the feasibility and usefulness of this environmentally friendly water treatment method by demonstrating its effectiveness.

**Keywords:** Methylene blue, Chitosan, Green citrus mold

Şerife PARLAYICI<sup>1</sup>  
Erol PEHLİVAN<sup>1</sup>



<sup>1</sup> Department of Chemical Engineering,  
Faculty of Engineering and Natural Sciences,  
Konya Technical University, Konya, Türkiye



### INTRODUCTION

Over 10,000 tons of dye are used annually in the textile industry worldwide; 10-15% of this quantity ends up in effluent.<sup>1,2</sup> The demand for sustainable and effective wastewater treatment systems has grown due to growing concerns about contamination of the environment. Synthetic dyes are one of the most dangerous types of pollution because of their enduring nature and detrimental impact on ecosystems. Methylene Blue (MB), a dye that is frequently used in printing and textile industries, is well-known to have toxicological effects. Therefore, it is critical to find economical and environmentally beneficial ways to reduce MB contamination.

Since the discharge of many types of solid and liquid waste into waterways poses a serious risk to the environment and the health of people, contamination by wastewater is a global concern. Because of their toxicity and durability, synthetic dyes like MB when released into wastewater streams can have negative consequences. MB, a heterocyclic aromatic chemical molecule with a long history of use in scientific and commercial applications, has attracted attention due to its potential for environmental cleanup. MB is explained by its versatility, its ability to act as a dye, drug and redox indicator. Researchers are looking into sustainable methods to get rid of these types of dyes and lessen their negative effects on the environment to solve this issue. MB, a synthetic dye widely utilized in a variety of industries including textiles, printing, and water treatment, is one specific contaminant of interest. It is well recognized that MB is hazardous to aquatic life and that releasing it into waterways without the necessary treatment can harm habitats.

Received 01.08.2024  
Accepted 03.09.2024  
Publication Date 10.10.2024

Corresponding author: Erol Pehlivan  
E-mail: erolpehlivan@gmail.com

Cite this article: Parlayıcı Ş, Pehlivan E. Removal of Hazardous Methylene Blue from Aqueous Solutions by Green Citrus Mold (*Penicillium digitatum*)@Chitosan Hydrogel Beads. *Pharmata*. 2024;4(4):89-101.



Content of this journal is licensed under a Creative Commons Attribution-Noncommercial 4.0 International License.

Ctsn, one of the most common polysaccharides in nature, is a biodegradable biopolymer molecule formed when chitin in the exoskeleton of crustaceans is deacetylated.<sup>3,4,5</sup> Deacetylating chitin yields chitosan, a white, viscoelastic polysaccharide that is both biodegradable and nontoxic. Ctsn removes pollutants by creating strong chemical connections with them and acting as an adsorbent and coagulant. Negatively charged compounds, like MB, are drawn to and bonded to by its positively charged amino groups, which causes the molecules to separate from the water. This is helpful in the general decontamination of wastewater in addition to helping to remove the dye. Ctsn is an excellent choice for adsorption-based activities because of its many advantageous characteristics, which include its high surface area, abundance of amino and hydroxyl groups, and cationic nature.<sup>6,7</sup> Ctsn, a biopolymer, offers favorable properties such as biodegradability and biocompatibility, making it an excellent candidate for adsorption studies. There are simple, non-toxic methods to synthesize chitosan hydrogel beads.

Utilizing Green citrus mold (GCM) (*Penicillium digitatum*), a form of green mold frequently seen on citrus fruits, in conjunction with a Ctsn composite is one effective strategy that has been researched. GCM, sometimes known as green citrus mold, is this interesting microbiological agent. This fungus is well-known for its part in food spoiling, but it also has metabolic and enzymatic properties that make it useful in a variety of biotechnological applications, such as the removal and degradation of contaminants from watery environments. Because of its resilience and versatility, it is a great choice for cleaning up pollution. GCM is a common post-harvest pathogen of citrus and has several intrinsic qualities that make it a good choice for adsorption methods, such as its low cost, abundance in nature and environmental friendliness. Food deterioration is frequently caused by penicillium fungus, particularly in fruits and vegetables. Typically, citrus is attacked by *Penicillium italicum* and GCM. GCM is more prone to developing rots than *Penicillium italicum*. The fruit wounds allow the fungi to spread their infection, although contact infection is also possible. Green mold GCM and blue mold (*Penicillium italicum*) are two of the post-harvest diseases that cause the most financial harm to the citrus fruit trade.<sup>8</sup>

Conventional physicochemical techniques for removing dyes from water include electrochemical, coagulation-flocculation, and adsorption.<sup>9</sup> The primary drawbacks of these techniques are their high prices and rapid sludge

regeneration. Consequently, the biological processes that decolorized and/or degrade these pigments might be effective strategies to reduce their negative effects.<sup>10</sup> Microorganisms have garnered significant interest in the cleanup of heavy metals due to their broad availability, inexpensive cost, and high sorption capability.<sup>11</sup>

GCM@Ctsn hydrogel beads combine to provide an innovative way to remove organic dyes from aqueous solutions, including MB. GCM can provide enhanced adsorption capacities when immobilized in Ctsn hydrogel beads due to the synergistic effects of the microbe and the biopolymer matrix. One possible strategy is to use fungal species such as GCM in combination with Ctsn. Crab shells are the source of Ctsn, a biopolymer that occurs naturally. It has garnered a lot of attention lately because of its many characteristics, which include biodegradability, non-toxicity, and a significant tendency to bond with pollutants. GCM@Ctsn combine to generate a hybrid material with enhanced pollution-removal capabilities.<sup>12</sup>

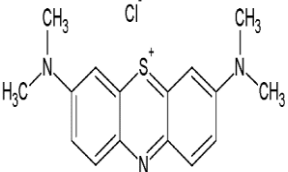
The aim of this study was to investigate the kinetic behavior, isotherms, and adsorption mechanism of MB elimination process by green citrus mold immobilized in Ctsn hydrogel beads. It is essential to comprehend the underlying basic processes of this adsorption system to optimize its performance and investigate its potential for practical application in wastewater treatment. The experimental setup involved the determination of various parameters such as initial MB concentration, contact time, pH, temperature, and adsorbent dosage to optimize the adsorption process. This paper describes an investigation into the effectiveness of this composite in removing MB dye from water and presents a potential environmentally friendly solution. The unique characteristics of both the green mould and chitosan significantly enhance their overall adsorption capabilities. In this composite, the remarkable binding properties of Ctsn and the high adsorption capacity of GCM are effectively coupled. Together, they work in concert to effectively remove MB from aqueous medium.

## METHODS

### Materials

Chitosan flakes (degree of deacetylation, DD = 75–85%) was purchased from Sigma-Aldrich Company. NaOH, HCl, and acetic acid were purchased from Merck Company. Methylene blue referred to as MB was purchased from Acros Organics (Table 1). All related chemicals used in the experiments were of analytical grade. In the preparation of the composite adsorbent, IKAMAG-RO15 model mechanical stirrer, Thermostated shaker of GFL 3033

**Table 1.** Main characteristics of tested MB

Structural formula	M (g.mol <sup>-1</sup> )	Molecular Formula
	319.85	C <sub>16</sub> H <sub>18</sub> ClN <sub>3</sub> S · xH <sub>2</sub> O
Physical Form	Solubility	
Crystalline Powder with Metal Luster	Solubility in water: soluble. Other solubilities: soluble in alcohol and chloroform, insoluble in ether	
Color	λ <sub>max</sub> (nm)	Storage temp.
Green powder	664	Room temp.

model, a pH meter (Orion 900S2) with glass electrode was used. UV-visible spectrophotometer (Schmadzu UV-1700) was used for the determination of MB ( $\lambda_{\max}$ : 664 nm). The FT-IR spectrum was recorded by a Bruker VERTEX 70 FT-IR spectrometer. Microstructure of the Adsorbent was examined using of scanning electron microscope (SEM, Nova Nano SEM 200, FEI Company).

### Synthesis of adsorbent

Green citrus mold (GCM) (*Penicillium digitatum*), a form of green mold frequently seen in citrus fruits, was obtained by keeping citrus fruits in a closed glass container for one month. It was dried at room temperature. The powder of the GCM was collected in a sealed sample tube (Figure 1). A 2% v/v acetic acid solution was used to dissolve 3 g of Ctsn, and the mixture was swirled for 24 hours to produce a transparent solution. After that, 1.5 g of dried GCM in powder form was added to the Ctsn solution and mixed for 5 hours to produce a homogenous suspension. To create composite spheres, a burette was used to drop the Ctsn@GCM mixture dropwise into a sodium hydroxide solution (600 mL methanol, 400 mL water, and 120 g of NaOH). They spent the night in a bath of NaOH. To get rid of extra acetic acid, the spheres were filtered and cleaned until the medium was neutral. The beads were stirred for 30 minutes at 60–70°C to observe the ionic crosslinking process with glutaraldehyde. The composite spheres were filtered, repeatedly cleaned in deionized water, dried at 60°C, and stored until needed after the reaction.

### Experiments

The batch-shaking adsorption technique was used to conduct experiments by varying temperature, adsorbent quantity, pH, concentration, and contact duration. For pH studies, the range of 2 to 8 was selected, and for temperature, the range of 25 to 45 degrees Celsius was chosen. Using a 500 ppm stock MB solution, solutions were produced at appropriate concentrations between 25 ppm and 300 ppm. The ranges of 0.5 g/L–3.0 g/L and 5 min–240 min were used to investigate the effects of adsorbent dose and contact duration, respectively. 0.1 M

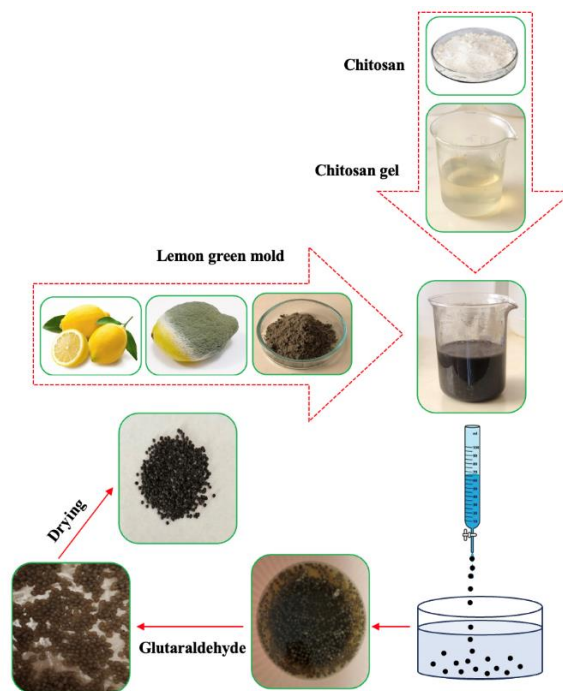


**Figure 1.** Schematic diagram of preparation of GCM@Ctsn beads.

HCl and 0.1 M NaOH were used to alter the pH. The samples were filtered and the residual MB concentration in the solution was computed after vigorous shaking for two hours. The concentration of dye in the solution phase was determined using a UV-Vis spectrophotometer. At 665 nm, the concentrations of MB in the solution phase were determined. Equations 1 and 2 were used to compute the equilibrium adsorption capacity ( $q_e$ ), which reflects the dye adsorption on the adsorbent. The chemical interactions between the dye molecules and the GCM@Ctsn beads will be investigated using Fourier-transform infrared spectroscopy (FT-IR). UV-vis spectrophotometry was used to analyze the treated solutions. The percentage of MB removed was computed using the following formula:<sup>13</sup>

$$q_e = (C_o - C_e) V/m \quad (1)$$

$$\% \text{ Adsorption} = C_o - C_e / C_o \times 100 \quad (2)$$

Where  $C_e$  is the equilibrium concentration of methylene blue and  $C_o$  is its starting concentration.

## RESULTS

### FT-IR analyses of GCM@Ctsn

The results obtained from FTIR analysis of GCM@Ctsn are shown in Figure 2. When the FT-IR spectra of GCM@Ctsn are examined, a wide absorption band in the range of  $3500-3800\text{ cm}^{-1}$  is shown with OH and NH stretching. Various C-H stretching at  $2921\text{ cm}^{-1}$ , C=H bond stretching (carbonyl group) at  $2357\text{ cm}^{-1}$ , amide I vibration band<sup>14</sup> at  $1642-1741\text{ cm}^{-1}$ , amide II vibration band at  $1542\text{ cm}^{-1}$ , various C-C-H, C-O-C, C-C-O bendings and C-C, C-O stretching vibrations between  $1800-1500\text{ cm}^{-1}$  were observed in the FT-IR spectrum.<sup>15</sup> The peaks at  $1741$ ,  $1642$ ,  $1542$ ,  $1398$ , and  $1238\text{ cm}^{-1}$  were assigned to the presence of aliphatic amines (C=O stretch), amines (N-H bend), and carboxylic acids (C-H bend, C-N stretch).<sup>16</sup> Furthermore, the peaks at  $1044\text{ cm}^{-1}$  correspond to the C-O-C stretch and the peaks at  $671\text{ cm}^{-1}$  correspond to the C-H bend planar vibrations of alkenes.

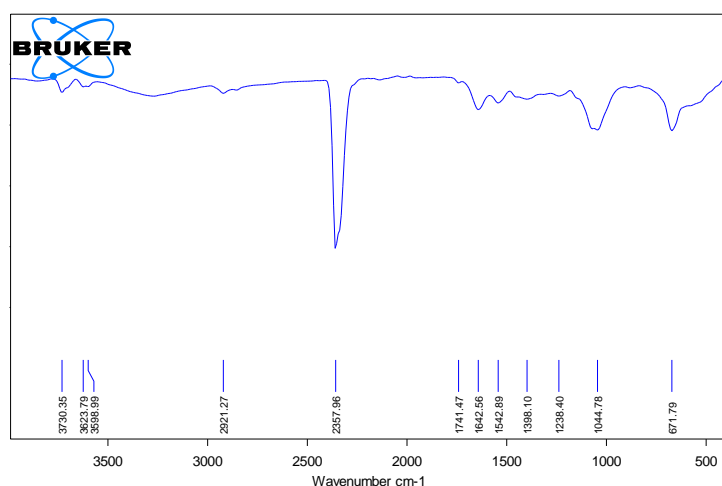


Figure 2. FTIR analysis of GCM@Ctsn

### SEM analyses of GCM@Ctsn

SEM analysis was performed to obtain information about the pores formed on the surface of the adsorbent surface morphology. SEM images of GCM@Ctsn before and after MB adsorption are shown in Figure 3. When the SEM images are examined, it is seen that the GCM@Ctsn composite has a spherical structure, its surface has an irregular, hollow, indented and protruding structure and there are cavities. Figure 3a shows SEM images of the adsorbent magnified at certain ratios. These pores show that it can be used as adsorbent. These pores in the bioadsorbent structure hold the MB dye inside and on the surface. After the adsorption process, it was observed that the spherical structure remained intact in SEM images. In

addition, as can be seen in Figure 3b, MB dye was coated on the pores, making the surface smooth. It was reported that the MB dye adsorption with eucalyptus biochars resulted in a smoother surface in SEM images.<sup>17</sup> Similar situation was observed for the adsorption of MB dye on GCM@Ctsn surface.

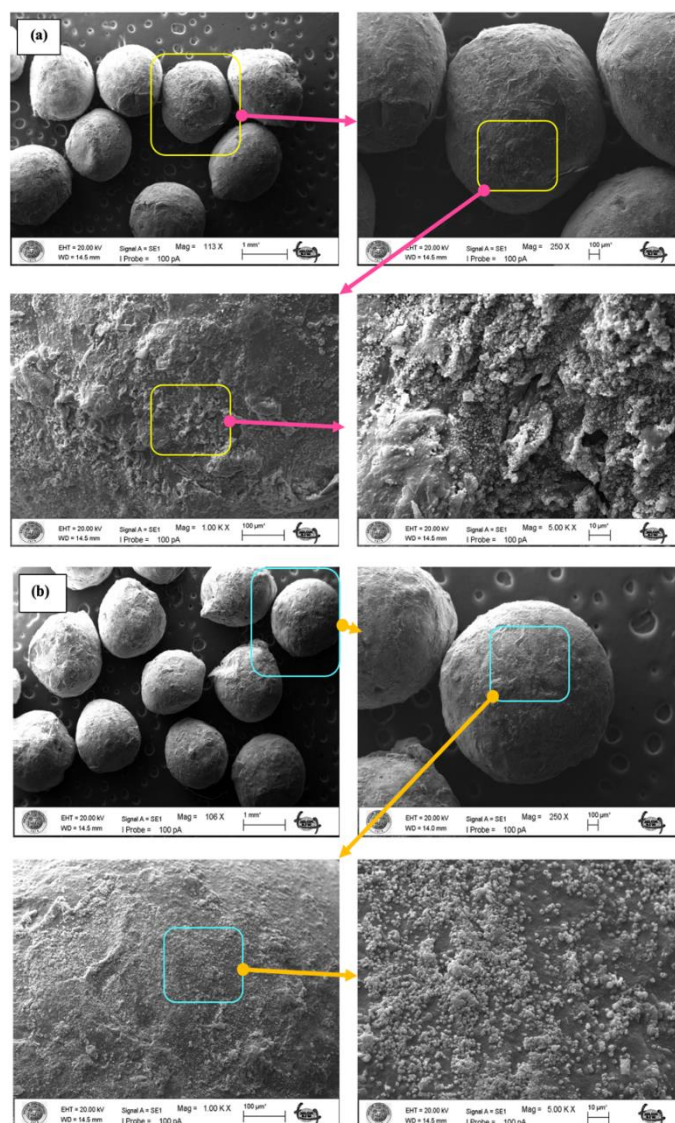
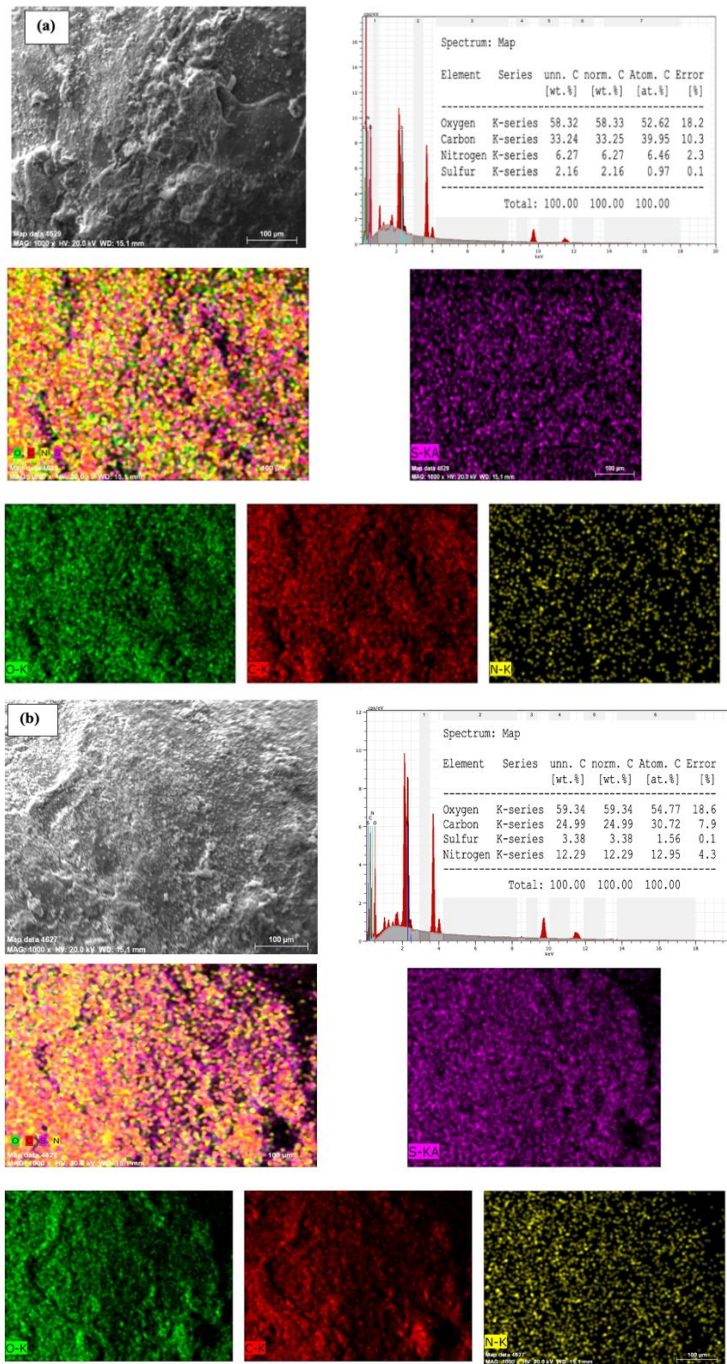


Figure 3. SEM images of GCM@Ctsn: (a) before and (b) after MB adsorption

### EDX analyses of GCM@Ctsn

Energy dispersive X-ray analysis (EDX) is a method used in scanning electron microscopy to characterize the elemental composition of a sample. EDX analysis results of GCM@Ctsn before and after adsorption are given in Figure 4. It shows that 58.32% O, 33.25% C, 6.27% N and 2.16% S were present on the biosorbent surface before adsorption. These values were determined as 59.34% O, 24.99% C, 12.29% N and 3.38% S after the adsorption process (Figure 4(b)). After the analysis, the reason for the increase in the ratio of N and S in the total amount is the

N and S in the chemical structure of the adsorbed MB molecule.



**Figure 4.** EDX analysis of GCM@Ctsn: (a) before and (b) after MB adsorption

#### Dye concentration effect and adsorption isotherms

Langmuir, Freundlich, Scatchard, D-R and Temkin isotherms are the most widely used adsorption isotherm models; each provides a distinct viewpoint on the adsorption phenomenon.<sup>18-22</sup> These isotherms provide important information about the mechanism and effectiveness of the adsorption process and are essential

for comprehending the behavior of MB molecules when they are adsorbed onto solid surfaces like GCM@Ctsn beads.

The Langmuir isotherm model assumes that there is no interaction between the molecules of the adsorbate and monolayer adsorption onto a homogenous surface. Langmuir isotherm model, the linear formula is defined as follows (Eq. 3):

$$C_e/q_e = 1/K_L q_m + C_e/q_m \quad (3)$$

$$R_L = 1/(1 + K_L C_0) \quad (4)$$

Heterogeneous surfaces and multilayer adsorption are made possible by the Freundlich isotherm. It explains the process of adsorption onto a surface with different capabilities and affinities. The Freundlich adsorption isotherm model is defined by Eq. 5.

$$\log q_e = \log K_F + 1/n \log C_e \quad (5)$$

The Scatchard isotherm is used to explain how molecules connect to surfaces that have several binding sites. It was initially created to investigate how compounds attach to surfaces in adsorbent structures.

The Scatchard model is expressed by Eq. (6).

$$q_e/C_e = Q_s K_s - q_e K_s \quad (6)$$

For modelling adsorption onto porous materials, another common model is the Dubinin-Radushkevich (D-R) isotherm. The D-R isotherm supports multilayer adsorption and accounts for the heterogeneity of the adsorbent surface.

The D-R isotherm model is expressed by Eq. (7)

$$\ln q_e = \ln q_m - \beta \varepsilon^2 \quad (7)$$

The Temkin isotherm accounts for the effects of interactions between the adsorbent and the adsorbate and assumes a linear decrease in adsorption energy with surface coverage. It provides insights into the energetics of the adsorption process and the interactions between the adsorbate and the adsorbent, although it might not be suitable for systems with strong chemical interactions. The Temkin isotherm model is defined by Eq. 8.

$$q_e = B \ln K_t + B \ln C_e \quad (8)$$

Measuring the difference in dye concentration in solution before and after treatment with the GCM@Ctsn beads allowed the removal efficiency of MB to be calculated. This was accomplished by measuring the amount of light absorbed by the dye using a UV-vis spectrophotometer.

Adsorption isotherms offer important insights into the connection between the MB concentration and the composite adsorption capability. Knowing these isotherms assists in eliminating MB by optimizing the process parameters. Plotting the quantity of MB adsorbed versus the equilibrium concentration allowed for the construction of the adsorption isotherms. Since the adsorption isotherms often displayed a characteristic shape corresponding with a Langmuir or Freundlich isotherm model, it was able to quantify the adsorption behavior and establish the maximum adsorption capacity. The adsorption behavior was analyzed using the Langmuir isotherm model.

The slope and intercept of the Langmuir isotherm equation were used to calculate the maximum adsorption capacity, also referred to as the Langmuir adsorption capacity ( $q_m$ ). In this investigation, the  $q_m$  value which indicates the adsorption effectiveness of the composite material was found to be rather high, indicating that MB was effectively removed. The maximum adsorption capacity, commonly known as the Langmuir adsorption capacity ( $q_m$ ), was determined using the slope and intercept of the Langmuir isotherm equation. A comparatively high  $q_m$  value was found suggesting the effective elimination of MB and the adsorption efficacy of the composite material. Furthermore, the kind of adsorption was ascertained by the use of a crucial parameter that was obtained from the Langmuir isotherm model: the separation factor, also referred to as the dimensionless equilibrium parameter ( $R_L$ ). The calculated  $R_L$  values in this investigation were within the range of 0 to 1, which indicates good adsorption and suggests that the method of adsorption was successful.<sup>23</sup> Removal efficiency is expected to rise, at least initially, with increasing MB concentrations because there are more dye molecules available for adsorption. However, further concentration improvement may not yield significant increases in efficiency once the adsorption sites on the composite surface are saturated.

Our results indicate that the removal efficiency of MB increased with increasing concentrations of MB. This suggests that higher initial concentrations of MB result in higher removal efficiency. It is important to note that the removal efficiency exhibited a diminishing rate of increase with higher MB concentrations. This could be due to the saturation of active sites available for adsorption on the GCM@Ctsn beads. As the concentration of MB surpasses the adsorption capacity, the removal efficiency tends to level off.

The concentrations of MB were measured at 25, 50, 100, 150, 200, 250, and 300 parts per million (ppm). It was blended for 120 minutes at 150 rpm, 25 °C, and a dosage of 2 g/L GCM@Ctsn beads using a shaker. The amount of dye that remained unadsorbed was calculated by measuring the absorbance of the UV-Vis. Spectrophotometer. Figure 5. shows the results of a study on the effects of concentration variations on adsorption.

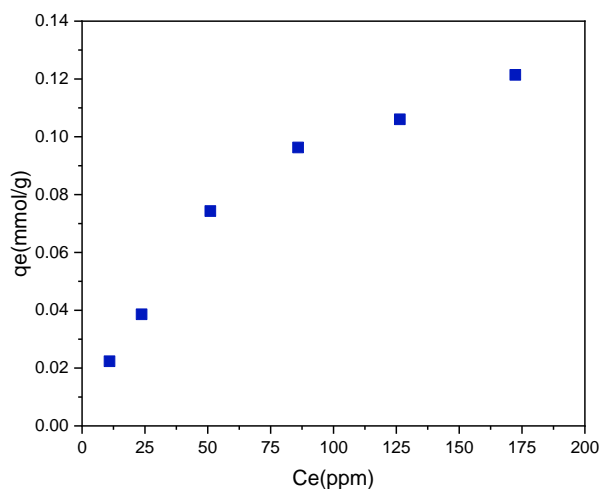
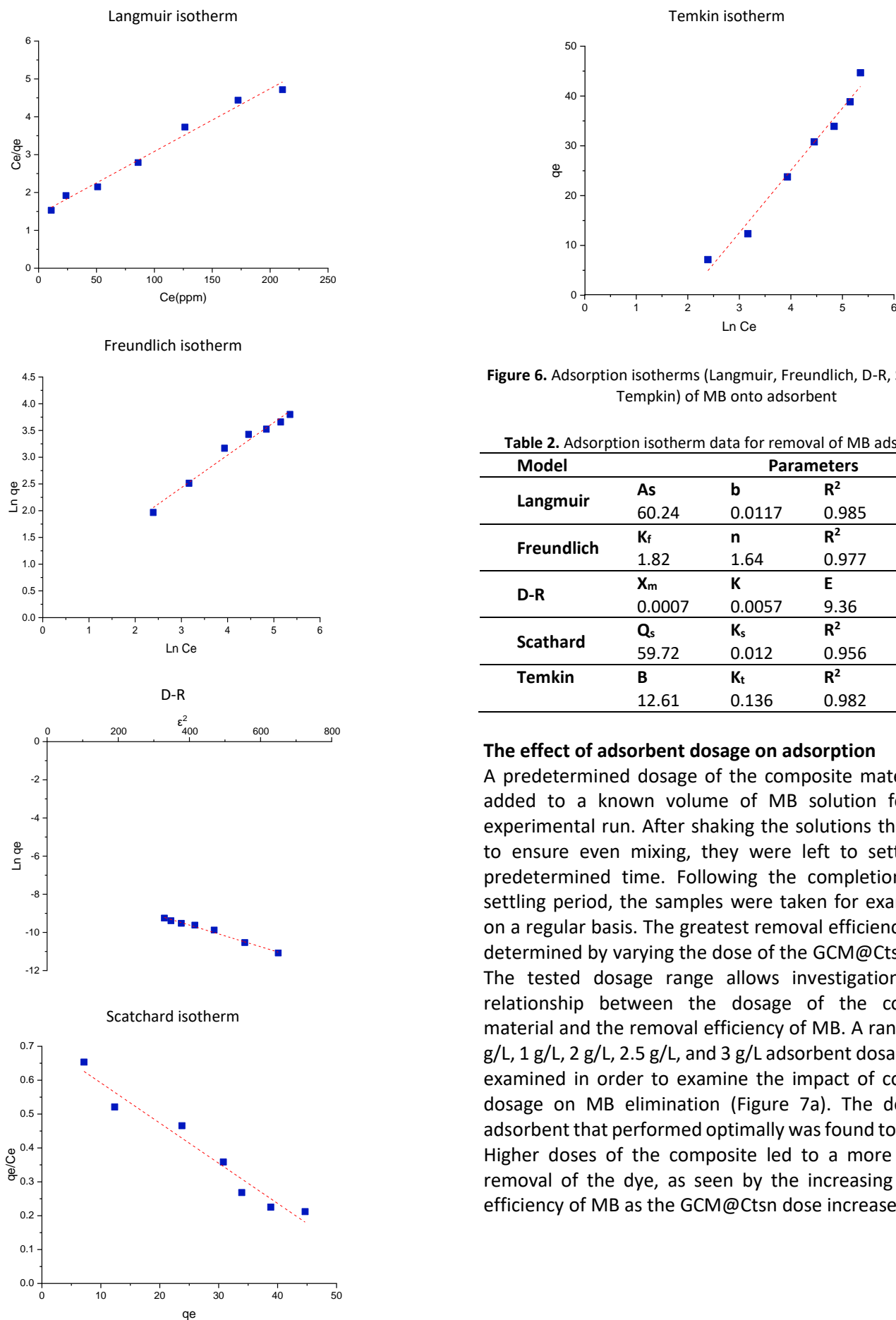


Figure 5. Influence of initial MB concentration

The determination of the interaction between adsorbate molecules and adsorbent surfaces largely depends on adsorption isotherms. Depending on the particulars of the system and the information being sought, an adsorption isotherm can be chosen to analyze the removal of dye from aqueous solutions employing adsorbents. Investigation of adsorption isotherms in the context of MB removal from aqueous solutions using GCM@Ctsn beads acting as adsorbents provides important information about the process efficiency and mechanism of adsorption. When the correlation coefficients of the isotherms were examined according to the data obtained in this study, it was seen that MB removal using GCM@Ctsn beads was more compatible with the Langmuir adsorption isotherm (Figure 6).  $Q_{max}$  value of GCM@Ctsn from Langmuir isotherm parameters was calculated as 60.24 mg/g (Table 2). Accordingly, we can say that adsorption for MB dyestuff occurs in specific homogeneous regions on GCM@Ctsn, and also that MB molecules are covered as a monolayer on the surface of GCM@Ctsn.



**Figure 6.** Adsorption isotherms (Langmuir, Freundlich, D-R, Scatchard, Temkin) of MB onto adsorbent

**Table 2.** Adsorption isotherm data for removal of MB adsorption

Model	Parameters			
Langmuir	$A_s$	$b$	$R^2$	$R_L$
	60.24	0.0117	0.985	0.632
Freundlich	$K_f$	$n$	$R^2$	
	1.82	1.64	0.977	
D-R	$X_m$	$K$	$E$	$R^2$
	0.0007	0.0057	9.36	0.987
Scatchard	$Q_s$	$K_s$	$R^2$	
	59.72	0.012	0.956	
Temkin	$B$	$K_t$	$R^2$	
	12.61	0.136	0.982	

### The effect of adsorbent dosage on adsorption

A predetermined dosage of the composite material was added to a known volume of MB solution for every experimental run. After shaking the solutions thoroughly to ensure even mixing, they were left to settle for a predetermined time. Following the completion of the settling period, the samples were taken for examination on a regular basis. The greatest removal efficiency can be determined by varying the dose of the GCM@Ctsn beads. The tested dosage range allows investigation of the relationship between the dosage of the composite material and the removal efficiency of MB. A range of 0.5 g/L, 1 g/L, 2 g/L, 2.5 g/L, and 3 g/L adsorbent dosages were examined in order to examine the impact of composite dosage on MB elimination (Figure 7a). The dosage of adsorbent that performed optimally was found to be 2 g/L. Higher doses of the composite led to a more efficient removal of the dye, as seen by the increasing removal efficiency of MB as the GCM@Ctsn dose increased.

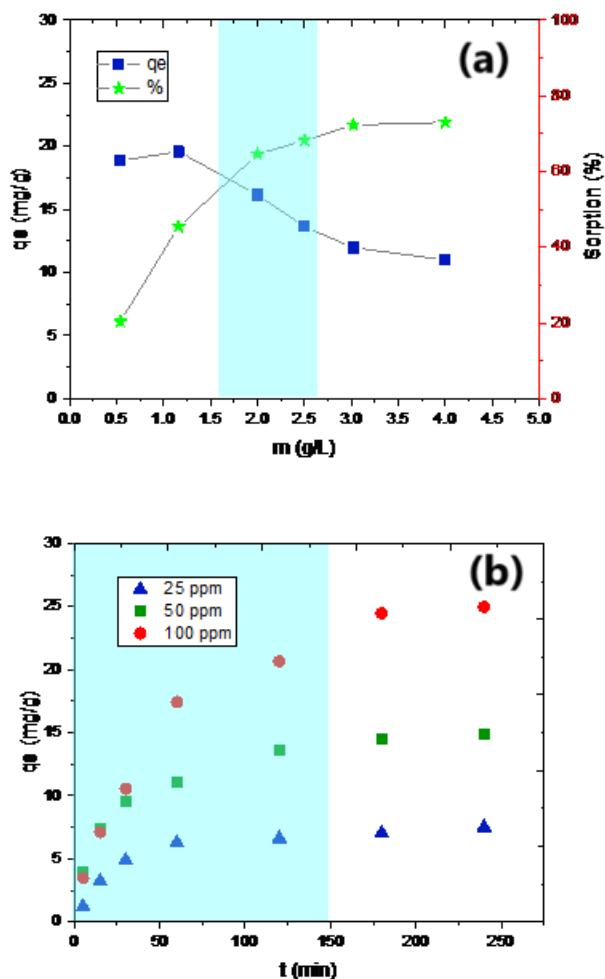


**Figure 7.** Adsorption of MB on the surface of GCM@Ctsn beads: (a) effect of adsorbent dosage, (b) effect of contact time

### The effect of contact time on adsorption

Temperature, pH, and the duration of the contact were found to have a significant impact on the adsorption of MB onto the GCM@Ctsn.<sup>24</sup> Knowing the relationship between contact time and dye adsorption is necessary to optimize both the design and performance of dye removal processes. It was found that as the duration of contact was examined, the adsorption capacity rose over time until reaching equilibrium. The length of time interactions is allowed to occur directly affects how effective the adsorption process is. Due to the large number of active sites available for adsorption on the surface of the GCM@Ctsn, the dye adsorption rate is usually high at first. However, as time passes, fewer vacant active sites remain, reducing the dye adsorption rate. This implies that the GCM@Ctsn needs enough time to draw out the dye from the solution. Longer contact times may increase adsorption capacity and improve removal efficiency, according to the data.

The efficiency of the adsorption process is directly impacted by the amount of time interactions are permitted to take place. The dye adsorption rate is often high at initially because the surface of the composite has a large number of active sites that are available for adsorption. But as time goes on, the number of unoccupied active sites decreases, which lowers the dye adsorption rate. The elimination percentage of MB improved steadily during the course of the contact duration. This suggests that the GCM@Ctsn was successfully saturating the dye molecules by adsorption. Higher clearance percentages were achieved because the extended contact time for more thorough adsorption.

At various contact durations (5, 15, 30, 60, 120, 180, and 240 min.), 2 g/L GCM@Ctsn dose, natural pH of the solution, 25 °C, and 150 ppm, the impact of contact time on MB adsorption was investigated (Figure 7b). Examining the Figure 7. reveals that in the first thirty minutes, the MB dye adsorption on the composite adsorbent sample grows quickly, and in the next 120 minutes, it nearly achieves equilibrium. The adsorption time was found to be 120 minutes for the time it took to achieve equilibrium.

### Effect of pH on adsorption

The pH of the solution is significant and a key factor in the dye removal processes because it influences the surface charge of the adsorbent and the dye molecule.<sup>25</sup> Comprehending this impact is crucial for customizing the adsorption procedure to attain optimal elimination efficacy. The solubility of the adsorbent and the surface charge of the contaminant are directly influenced by pH. Near-neutral pH values yielded the best acceptance effectiveness. The results show that the GCM@Ctsn works best in neutral environments, which means it can be used in situations where controlling pH is difficult. The surface charge of adsorbent varies as the pH of the solution rises. GCM@Ctsn beads contain positively charged surfaces at low pH levels. The dissociation of ionizable groups in the adsorbents causes the surface charge to get more negative as the pH rises. The electrostatic interactions between the molecules of the MB dye and the adsorbent are impacted by this charge reversal process. Consequently, the pH of the solution affects the adsorption capacity.

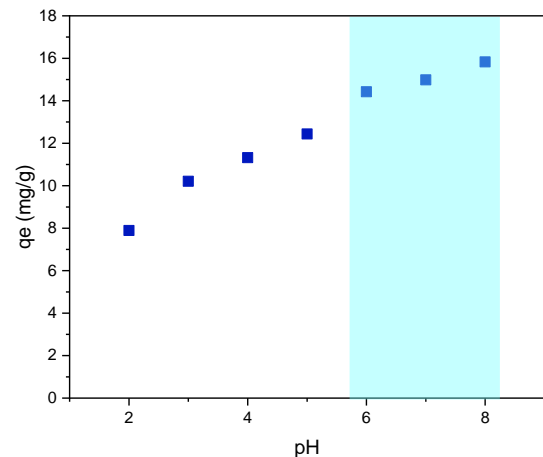
Because different functional groups on the surface of an adsorbent are ionized and protonated as the pH of a solution changes, this has an impact on the adsorbent's surface charge. The surfaces of the GCM@Ctsn beads, which are utilized as the adsorbent, have functional groups like carboxyl, amino, and hydroxyl groups. Depending on the pH of the solution, these groups may

ionize or protonate, altering the surface charge. The solubility of MB in water is influenced by pH. The cationic form of MB predominates at lower pH levels, whereas the anionic form is prevalent at higher pH values. The ionic state change of the dye has an impact on how well it will bind to the adsorbent. By adjusting pH, the ionic state and surface charge of MB may be changed, which maximizes the adsorption capacity. The deprotonation of functional groups causes the adsorbent's surface charge to become extremely negative under high pH levels, or alkaline circumstances. The MB molecules may be repelled by this negatively charged surface, greatly reducing their adsorption ability. The adsorption process may change from electrostatic attraction to other mechanisms, such as hydrophobic or  $\pi$ - $\pi$  interactions, in alkaline circumstances. Lower removal efficiency for MB from the solution may arise from these other processes, which might not be as effective as electrostatic attraction. Changes in pH eventually impact the solubility of MB, the availability of binding sites, and the electrostatic attraction between the adsorbent and MB, which determines the efficacy of the adsorption process.

There are several reasons for the improved adsorption kinetics attained with this composite material. First off, GCM@Ctsn work together to produce a structure that is more porous and has a larger surface area. Because of its porous nature, which offers plenty of locations for adsorption, the adsorbent can interact with more dye molecules. Second, a variety of mechanisms, including electrostatic attractions, hydrogen bonds, and  $\pi$ - $\pi$  interactions, are used by the functional groups in chitosan, such as amine and hydroxyl groups, to interact with the methylene blue dye. The enhanced adsorption capacity and kinetics of the composite material are a result of these interactions.

Using the GCM@Ctsn combination, a number of studies were carried out to ascertain the ideal pH range for the elimination of MB. Testing was done at several pH levels, from acidic to alkaline, and the effectiveness of MB removal was evaluated at each one. The experimental outcomes gathered at pH 2, 3, 4, 5, 6, 7, and 8 to observe the effect of pH on the adsorption of MB dye on the adsorbent are presented in Figure 8. The initial pH values of the solutions were found to be 6.0 for MB. It is necessary to do in-depth research on the effects of solution pH changes on MB adsorption. The pH range, between pH 6 and pH 8, was shown to be the optimal range for attaining optimum removal effectiveness. MB adsorption generally decreases noticeably at low pH levels in the solution. This process happens because the

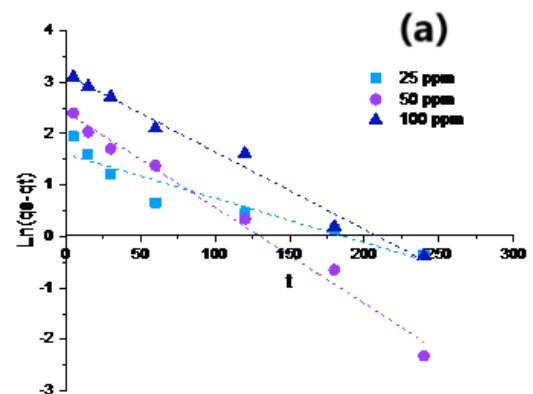
adsorbent's surface becomes more positively charged in an acidic environment, which causes the cationic dye molecules to repel one another electrostatically. Consequently, the overall adsorption capacity diminishes as the MB's affinity for the GCM@Ctsn surface declines. This result emphasizes how crucial pH regulation is to maximizing the effectiveness of dye removal procedures.



**Figure 8.** Effect of pH on the adsorption of MB on the surface of GCM@Ctsn beads

### Adsorption kinetics

The study of how quickly and effectively a substance adsorbs or sticks to the surface of a solid material is known as adsorption kinetics (Figure 9). A common dye used in many different businesses is MB, which has been linked to possible environmental impacts. One popular kinetic model for explaining the adsorption process onto solid surfaces is the Elovich model. It is appropriate for a range of adsorption systems since it integrates both chemical and physical adsorption pathways (Table 3).



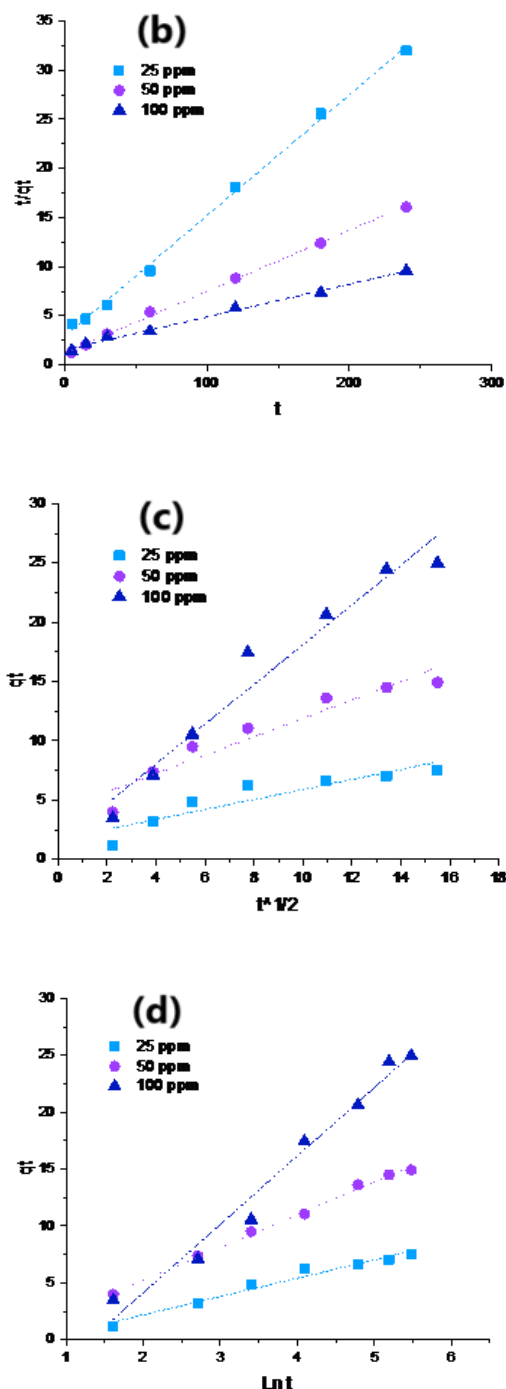


**Figure 9.** Kinetic models (pseudo-first-order kinetic model (a) pseudo-second-order kinetic model (b) intra-particle diffusion model (c) and elovich model (d)) for MB adsorption onto GCM@Ctsn beads

$$\ln(q_e - q_t) = \ln q_e - k_1 t \quad (9)$$

$$\frac{1}{q_t} = \frac{1}{k_2 q_e^2} + \frac{1}{q_e t} \quad (10)$$

Elovich model was expressed using the following (Eq.11):

$$q_t = \frac{\ln \alpha \beta}{\beta} + \frac{\ln t}{\beta} \quad (11)$$

Weber and Morris formulate the intra-particle diffusion model to locate the migration of adsorbates from the surface of adsorbent into its internal pores because of stirring process as follows (Eq. 12):

$$q_t = k_{id} t^{0.5} + C \quad (12)$$

**Table 3.** Kinetic model parameter for MB removal

Kinetics modeling	Parameters	$C_0$ (ppm)	
Pseudo First-order	$q_e \text{ exp}$	25	8.2
		50	15.1
		100	25.7
	$k_1$	25	0.0086
		50	0.0187
		100	0.015
	$q_e$	25	4.99
		50	11.39
		100	23.38
	$R^2$	25	0.900
50		0.987	
100		0.985	
Pseudo Second- order	$k_2$	25	0.0052
		50	0.0031
		100	0.0007
	$q_e$	25	8.13
		50	16.05
		100	29.94
	$R^2$	25	0.998
		50	0.998
		100	0.995
	Elovich	$\alpha$	25
50			2.42
100			0.85
$\beta$		25	0.17
		50	0.35
		100	0.62
$R^2$		25	0.976
		50	0.996
		100	0.969
Intraparticle diffusion		$k_{id}$	25
	50		0.78
	100		0.42
	$C$	25	1.34
		50	4.12
		100	1.68
	$R^2$	25	0.956
		50	0.917
		100	0.836

### Thermodynamics of adsorption

Thermodynamics offers insightful information on the viability and energy of the method of adsorption. Understanding the thermodynamics of adsorption is essential to optimizing the efficiency and design of adsorption. Elevated temperatures resulted in an increased removal efficiency, subsequently impacting the adsorption capacity of the composite material. The calculation and evaluation of many thermodynamic parameters, including enthalpy ( $\Delta H^\circ$ ), entropy ( $\Delta S^\circ$ ), and Gibbs free energy ( $\Delta G^\circ$ ), are part of the investigation of thermodynamics in adsorption. The spontaneity and directionality of the adsorption process may be assessed using these parameters.

An endothermic reaction, in which the adsorbate is preferred at higher temperatures, is indicated by a positive  $\Delta H^\circ$ . Regarding the adsorption of MB by the composite, a positive  $\Delta S^\circ$  value indicates increased disorder during the adsorption procedure. This suggests that the adsorption of MB onto the composite surface results in a more random distribution of molecules, which increases the overall thermodynamic viability of the process. Conversely, a negative  $\Delta H^\circ$  denotes a more advantageous exothermic reaction at lower temperatures. The type of bonding or forces at play during the adsorption process may be ascertained with the support of the enthalpy change. Gibbs free energy ( $\Delta G^\circ$ ) is a fundamental thermodynamic principle that is crucial to adsorption. The energy is available to act as a chemical reaction or physical process is represented as Gibbs-free energy. The adsorption process may be classified as spontaneous ( $\Delta G^\circ < 0$ ) or non-spontaneous ( $\Delta G^\circ > 0$ ) based on the change in Gibbs free energy ( $\Delta G^\circ$ ).

The impact of temperature on MB adsorption on the adsorbent surface was investigated at 25°, 35°, and 45°C. The results of the experiment are given in Table 4. The graphic illustrates how the amount of MB adsorbed on the adsorbent surface drops as temperature rises.

$$\Delta G^\circ = -RT \ln K_c \quad (13)$$

$$\ln K_c = \frac{\Delta S^\circ}{R} - \frac{\Delta H^\circ}{RT} \quad (14)$$

**Table 4.** Thermodynamic parameters for adsorption of MB onto composite bead

$\Delta S^\circ$ (J K <sup>-1</sup> mol <sup>-1</sup> )	$\Delta H^\circ$ (J mol <sup>-1</sup> )	$\Delta G^\circ$ (J mol <sup>-1</sup> )			R <sup>2</sup>
		T=298.15K	T=308.15K	T=318.15K	
-9.62	-3505.81	-637.45	-541.25	-445.04	0.986

### Recycling efficiency

The regenerative nature of the GCM@Ctsn is one of its benefits. By desorbing the MB molecules, the composite may be readily renewed after it has reached its adsorption capacity. This characteristic makes reusing possible. The adsorbents' recyclability was tested over five cycles (Figure 10). The dye-loaded adsorbent was washed in ethanol to desorb dyes after each operation. Following an overnight drying process at 50°C to eliminate any remaining moisture, the regenerated samples were preserved for use in later cycles.

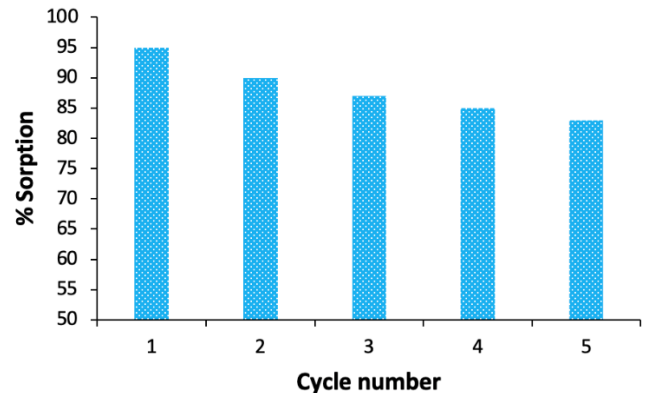


**Figure 10.** Desorption efficiency after recycle use

### Comparison with other adsorbents

The selection of an adsorbent should take into account various criteria, not only its capacity but also its practical usage, cost of preparation, availability, and raw materials utilized in its synthesis. Numerous studies have examined the usage of various adsorbents in the removal of MB from aqueous solutions in the literature. Table 5 presents an analysis of the maximum adsorption capabilities of several adsorbents from multiple investigations conducted under optimal conditions as a consequence of these studies. The adsorption capacity of GCM@Ctsn was found to be in line with the literature when compared to the given references.

### DISCUSSION

This article details an investigation on the composite's ability to remove MB dye from water as well as a potential environmentally friendly replacement. The adsorption capacity of GCM@Ctsn was greatly impacted by the medium's initial pH of 6.0. The Langmuir model was consistent with the adsorption results, which showed that a monolayer adsorption had taken place. It was demonstrated that the experimental results agreed with the PSO model. The existence of MB molecules and their uniform coating of the composite were validated by FT-IR and SEM analyses.

**Table 5.** Comparison of adsorption capacities of different adsorbents for MB removal

Adsorbent	q <sub>e</sub> (mgg <sup>-1</sup> )	Ref.
Chitosan-nSiO <sub>2</sub> nanocomposites	31.34	[26]
nanoTiO <sub>2</sub> -chitosan-plum kernel shell	86.96	[27]
Fe <sub>3</sub> O <sub>4</sub> /graphene/chitosan nanocomposite	94.16	[28]
Magnetic alginate-biochar from acorn cups	52.63	[25]
Chitosan magnetic composite microspheres	33.60	[29]
Lemongrass leaves	43.16	[30]
Magnetized chitosan nanocomposite	76.34	[31]
Chitosan/k-carrageenan/acid-activated bentonite composite membranes	18.80	[32]
Fe-modified banana peel	28.1	[33]
GCM@Ctsn	60.24	<i>This study</i>

The results of this study may aid in the development of long-lasting and efficient techniques for eliminating MB and other contaminants of a similar nature from water sources. Moreover, this research can open the door to affordable and environmentally friendly remedies to water contamination by employing widely accessible and sustainable ingredients like chitosan and *Penicillium digitatum*. Removing MB from aqueous solutions by using this composite material in wastewater treatment can help reduce water pollution caused by the textile industry. It also has the potential to be used in environmental remediation, helping to purify contaminated soil and water from dye contaminants.

The adsorption capability of the composite was shown to rise with greater MB concentrations, suggesting that the composite is successful in eliminating MB from polluted water, according to the data. Furthermore, the composite material was shown to adhere to the Langmuir model, indicating monolayer adsorption behavior, as indicated by the adsorption isotherms. The amount of time required for adsorption to reach equilibrium was found to be 120 minutes. Chemisorption, electrostatic attraction and pore filling are the prominent mechanisms for MB removal. The maximum adsorption capacity was found to be 60.24 mg/g. Moreover, pH had a significant effect on adsorption efficiency, and 6.0 was the most favorable pH value. Thermodynamic properties showed that the adsorption process was endothermic and spontaneous.

**Peer-review:** Externally peer-reviewed.

**Author Contributions:** Concept - AG; Design - AG, AAF; Supervision - AG; Resources - AG, BSK, HE; Materials - AG; Data Collection and/or Processing - AAG, BSK, HE; Analysis and/or Interpretation - AAG, BSK, HE; Literature Search - AAG, BSK, HE; Writing Manuscript - AAG, BSK, HE; Critical Review - AG.

**Conflict of Interest:** The authors have no conflicts of interest to declare.

**Financial Disclosure:** This study was funded by the Scientific and Technological Research Council of Turkey (TUBITAK) ARDEB 2209-A (Project code: 1919B012318796).

## REFERENCES

- Saratale RG, Saratale GD, Chang JS, Govindwar SP. Bacterial decolorization and degradation of azo dyes: A review. *J Taiwan Inst Chem Eng.* 2011;42(1):138–157. [\[CrossRef\]](#)
- Pereira L, Alves M. Dyes—environmental impact and remediation. *Environ Protec Strat Sustain Develop.* 2012;111-162. [\[CrossRef\]](#)
- Satitsri S, Muanprasat C. Chitin and chitosan derivatives as biomaterial resources for biological and biomedical applications. *Molecules.* 2020;25(24):5961. [\[CrossRef\]](#)
- Shahbaz U, Basharat S, Javed U, Bibi A, Yu XB. Chitosan: a multipurpose polymer in food industry. *Polym Bull.* 2023;80(4):3547–3569. [\[CrossRef\]](#)
- Strnad S, Zemljič LF. Cellulose–chitosan functional biocomposites. *Polymers.* 2023;15(2):425. [\[CrossRef\]](#)
- Perumal S, Atchudan R, Yoon DH, Joo J, Cheong W. Spherical chitosan/gelatin hydrogel particles for removal of multiple heavy metal ions from wastewater. *Ind Eng Chem Res.* 2019;58:9900–9907. [\[CrossRef\]](#)
- Thambiliyagodage C, Jayanetti M, Mendis A, et al. Recent advances in chitosan based applications. a review. *Materials.* 2023;16(5):2073. [\[CrossRef\]](#)
- Bhatta UK. Alternative management approaches of citrus diseases caused by *Penicillium digitatum* (green mold) and *Penicillium italicum* (blue mold). *Front Plant Sci.* 2022;12:833328. [\[CrossRef\]](#)
- Collivignarelli MC, Abbà A, Miino MC, Damiani S. Treatments for color removal from wastewater: State of the art. *J Environ Manag.* 2019;236:727–745. [\[CrossRef\]](#)
- Garg N, Garg A, Mukherji S. Eco-friendly decolorization and degradation of reactive yellow 145 textile dye by *Pseudomonas aeruginosa* and *Thiosphaera pantotropha*. *J Environ Manag.* 2020;263:110383. [\[CrossRef\]](#)
- Shi F, Liu ZG, Li JL, et al. Alterations in microbial community during the remediation of a black-odorous stream by acclimated composite microorganisms. *J Environ Sci.* 2022;118:181–193. [\[CrossRef\]](#)
- Singh J, Sharma P, Mishra V. Simultaneous removal of copper, nickel and zinc ions from aqueous phase by using mould. *Inter J Environ Sci Technol.* 2023;20(2):1937–1950. [\[CrossRef\]](#)
- Lafi R, Montasser I, Hafiane A. Adsorption of congo red dye from aqueous solutions by prepared activated carbon with oxygen-containing functional groups and its regeneration. *Adsorpt Sci Technol.* 2019;37(1-2):160–181. [\[CrossRef\]](#)
- Kurç MA, Güven K, Korcan E, Güven A, Malkoc S. Lead biosorption by a moderately halophile *Penicillium* sp. isolated from çamalti saltern in Turkey. *Anadolu University J Sci Technol C-Life Sci Biotechnol.* 2016;5(1):13-22. [\[CrossRef\]](#)
- Ünlü CH, Pollet E, Avérous L. Original macromolecular architectures based on poly( $\epsilon$ -caprolactone) and poly( $\epsilon$ -thiocaprolactone) grafted onto chitosan backbone. *Inter J Mol Sci.* 2018;19 (12):3799. [\[CrossRef\]](#)

16. Preethi S, Abarna K, Nithyasri M, et al. Synthesis and characterization of chitosan/zinc oxide nanocomposite for antibacterial activity onto cotton fabrics and dye degradation applications. *Int J Biol Macromol*. 2020;164:2779-2787. [\[CrossRef\]](#)
17. Dawood S, Sen TK, Phan C. Adsorption removal of Methylene Blue (MB) dye from aqueous solution by bio-char prepared from *Eucalyptus sheathiana* bark: kinetic, equilibrium, mechanism, thermodynamic and process design. *Desal Water Treat*. 2016;57(59):28964-28980. [\[CrossRef\]](#)
18. Langmuir I. The constitution and fundamental properties of solids and liquids. *J Franklin Inst*. 1917;183(1):102–105.
19. Freundlich H. Über die biosorption in lasungen. *J Phy Chem*. 1906;57:385–470.
20. Scatchard G. The attractions of proteins for small molecules and ions. *Ann N Y Acad Sci*. 1949;51(4):660–672.
21. Dubinin MM, Radushkevich LV. Equation of the characteristic curve of activated charcoal. *Proc Acad Sci USSR Phys Chem Sect*. 1947; 55:331–333.
22. Temkin M, Pyzhev V. Recent modifications to Langmuir isotherms. *Acta Physicochim USSR*. 1940;12:217–222.
23. Parlayıcı Ş, Yar A, Pehlivan E, Avcı A. ZnO-TiO<sub>2</sub> doped polyacrylonitrile nano fiber-Mat for elimination of Cr (VI) from polluted water. *J Anal Sci Technol*. 2019;10:1-12. [\[CrossRef\]](#)
24. Parlayıcı Ş, Pehlivan E. Fast decolorization of cationic dyes by nano-scale zero valent iron immobilized in sycamore tree seed pod fibers: kinetics and modelling study. *Int J Phytorem*. 2019;21(11):1130–1144. [\[CrossRef\]](#)
25. Parlayıcı Ş, Pehlivan E. An ecologically sustainable specific method using new magnetic alginate-biochar from acorn cups (*Quercus coccifera* L.) for decolorization of dyes. *Polym Bull*. 2023;80(10):11167–11191. [\[CrossRef\]](#)
26. Bhattacharya S, Bar N, Rajbansi B, Das SK. Adsorptive elimination of methylene blue dye from aqueous solution by chitosan-n SiO<sub>2</sub> nanocomposite: Adsorption and desorption study, scale-up design, statistical, and genetic algorithm modeling. *Environ Prog Sustain Energy*. 2024;43(2):e14282. [\[CrossRef\]](#)
27. Pehlivan E, Parlayıcı Ş. Fabrication of a novel biopolymer-based nanocomposite (nanoTiO<sub>2</sub>-chitosan-plum kernel shell) and adsorption of cationic dyes. *J Chem Technol Biotechnol*. 2021;96(12):3378–3387. [\[CrossRef\]](#)
28. Tran HTT, Hoang LT, Tran HV. Electrochemical synthesis of graphene from waste discharged battery electrodes and its applications to preparation of graphene/fe<sub>3</sub>o<sub>4</sub>/chitosan-nanosorbent for organic dyes removal. *Z Anorgan Allg Chem*. 2022;648(3):e202100313. [\[CrossRef\]](#)
29. Yan H, Li H, Yang H, Li A, Cheng R. Removal of various cationic dyes from aqueous solutions using a kind of fully biodegradable magnetic composite microsphere. *Chem Eng J*. 2013;223:402–411. [\[CrossRef\]](#)
30. Zein R, Purnomo JS, Ramadhani P, Alif MF, Safni S. Lemongrass (*Cymbopogon nardus*) leaves biowaste as an effective and low-cost adsorbent for methylene blue dyes removal: isotherms, kinetics, and thermodynamics studies. *Sep Sci Technol*. 2022;57(15):2341–2357. [\[CrossRef\]](#)
31. Mashkoo F, Nasar A, Jeong C. Magnetized chitosan nanocomposite as an effective adsorbent for the removal of methylene blue and malachite green dyes. *Biomass Conv Bioref*. 2024;14:313–325. [\[CrossRef\]](#)
32. Ulu A, Alpaslan M, Gultek A, Ates B. Eco-friendly chitosan/κ-carrageenan membranes reinforced with activated bentonite for adsorption of methylene blue. *Mater Chem Phys*. 2022;278:125611. [\[CrossRef\]](#)
33. Çatlıoğlu F, Akay S, Turunç E, et al. Preparation and application of Fe-modified banana peel in the adsorption of methylene blue: process optimization using response surface methodology. *Environ Nanotechnol Monit Manag*. 2021;16:100517. [\[CrossRef\]](#)